Simulation-Based Analysis of Feeder Operation with Different PV Smart Inverter Functions on an Actual Distribution System

Preprint

Jiyu Wang, Harsha Padullaparti, Murali Baggu, and Martha Symko-Davies

National Renewable Energy Laboratory

Presented at the 2024 IEEE PES T&D Conference & Exposition
Anaheim, California
May 6–9, 2024

NREL is a national laboratory of the U.S. Department of Energy
Office of Energy Efficiency & Renewable Energy
Operated by the Alliance for Sustainable Energy, LLC

This report is available at no cost from the National Renewable Energy Laboratory (NREL) at www.nrel.gov/publications.

Contract No. DE-AC36-08GO28308

Conference Paper
NREL/CP-5D00-87285
September 2024

Simulation-Based Analysis of Feeder Operation with Different PV Smart Inverter Functions on an Actual Distribution System

Preprint

Jiyu Wang, Harsha Padullaparti, Murali Baggu, and Martha Symko-Davies

National Renewable Energy Laboratory

Suggested Citation
Wang, Jiyu, Harsha Padullaparti, Murali Baggu, and Martha Symko-Davies. 2024. *Simulation-Based Analysis of Feeder Operation with Different PV Smart Inverter Functions on an Actual Distribution System: Preprint*. Golden, CO: National Renewable Energy Laboratory. NREL/CP-5D00-87285. https://www.nrel.gov/docs/fy24osti/87285.pdf.

NREL is a national laboratory of the U.S. Department of Energy
Office of Energy Efficiency & Renewable Energy
Operated by the Alliance for Sustainable Energy, LLC

This report is available at no cost from the National Renewable Energy Laboratory (NREL) at www.nrel.gov/publications.

Contract No. DE-AC36-08GO28308

Conference Paper
NREL/CP-5D00-87285
September 2024

National Renewable Energy Laboratory
15013 Denver West Parkway
Golden, CO 80401
303-275-3000 • www.nrel.gov

NOTICE

This work was authored by the National Renewable Energy Laboratory, operated by Alliance for Sustainable Energy, LLC, for the U.S. Department of Energy (DOE) under Contract No. DE-AC36-08GO28308. Funding provided by U.S. Department of Energy Office of Electricity and by California's Electric Program Investment Charge (EPIC) Program in San Diego Gas & Electric Company under a cooperative research-and-development agreement (CRADA) # CRD-17-712. The views expressed herein do not necessarily represent the views of the DOE or the U.S. Government.

Cover Photos by Dennis Schroeder: (clockwise, left to right) NREL 51934, NREL 45897, NREL 42160, NREL 45891, NREL 48097, NREL 46526.

Simulation-Based Analysis of Feeder Operation with Different PV Smart Inverter Functions on an Actual Distribution System

Jiyu Wang, Harsha Padullaparti, Murali Baggu, Martha Symko-Davies
National Renewable Energy Laboratory (NREL), Golden, Colorado.
Jiyu.Wang@nrel.gov; HarshaVardhana.Padullaparti@nrel.gov

***Abstract*— High penetration of photovoltaics (PV) in distribution feeders can cause problems, such as overvoltage, reverse power flow, and large net load changes. Traditional voltage regulation devices, such as capacitors and voltage regulators, can solve some of these problems but might have some delays. Today, smart inverters are gradually being used to provide voltage regulation and frequency support in distribution systems. Different smart inverter settings have been recommended in various rules and standards; however, the potential benefits and their impacts on distribution system operation are not well compared and studied. This paper presents a comparison of different smart inverter settings as applied to a distribution system. An actual feeder model from San Diego Gas & Electric Company is used to conduct the simulation. Additionally, a load disaggregation method is proposed to disaggregate the load and PV profile for each load location using advanced metering infrastructure net load measurements. Then, different smart inverter settings are applied to the PV systems in the feeder, and the simulation results are compared. The results show that the implementation of specific functions of smart inverters can reduce voltage exceedances, and the utility can determine the specific inverter setting based on its operational requirements.**

***Index Terms*— Distribution system, photovoltaic (PV), smart grid, smart inverter, voltage exceedance.**

I. Introduction

To reduce emissions from traditional power resources, it is important to replace fossil-fueled generation with renewable generation resources, such as solar [1]. In recent years, the penetration of both residential and commercial buildings' rooftop photovoltaic (PV) systems has been increasing rapidly [2]. The power generation from these PV systems can help to supply demand in the distribution system and therefore reduce the required amount of fossil fuel; however, PV systems can cause operational issues in distribution systems, especially at high penetration levels [3-7]. Traditional voltage regulation devices—such as load tap changers (LTCs), voltage regulators, and switched capacitor banks—can help regulate the voltages to some extent [8]; however, because these devices are electromechanical, they cannot offer a fast response needed to handle the fast voltage dynamics resulting from the PV generation variability. This shortcoming is particularly evident on cloudy and partially cloudy days because the PV power outputs change rapidly [9]. Further, the customer loads, which are often located far from the LTC and capacitor banks, could still experience voltage problems during the peak load or peak PV generation period because of the large voltage drops across the lines [10].

PV smart inverters are being used to regulate the voltages in distribution systems to provide the necessary real and reactive power support to mitigate voltage violations [11]. Smart inverters can be defined as inverters with advanced control functions [12]. Operators can set these devices to the desired real and reactive power outputs to compensate for the voltage fluctuations and exceedances [13]. Nevertheless, determining the appropriate PV smart inverter settings is complex because it is possible to implement numerous inverter settings on a given smart inverter [14]. This demonstration tested the performance of different smart inverter settings available in the standards and those of interest to utilities on an actual electric utility distribution system. The studied smart inverter settings include the settings recommended in California Rule 21 [15]; Hawaii Rule 14 [16]; IEEE 1547 [17]; and the custom settings of interest: Rule 21 with no deadband, hockey stick, and volt-volt ampere reactive (var)-watt control.

Rule 21 is an interconnection tariff levied by the California Public Utilities Commission that sets rules for the performance, function, metering, and communications of generation and storage facilities [15]. Hawaiian Electric is one of the first U.S. utilities to require distributed energy resource (DER) inverters to perform volt-var control, and the settings are defined in Rule 14 [16]. IEEE 1547-2018 is the IEEE standard for the interconnection and interoperability of DERs [17]. This standard lists the technical specifications for the interconnection and interoperability between utility electric power systems and DERs, such as PV generation [18]. Rule 21

without deadband uses the basic settings of the Rule 21 curve, but there is no deadband for the inverter to output 0% reactive power. The first custom setting of interest, referred to as 'Custom setting 1 (Hockey Stick 1)' in this paper, uses the basic settings of the Rule 21 curve, but there is no compensation in the low-voltage region. 'Custom setting 2 (Hockey Stick 2)' is similar to the setting of Hockey Stick 1, but it has a deeper reactive power absorption. The volt-var-watt setting is using the volt-var and volt-watt curve from Rule 21 [19]. The real power output will first be determined by the nodal voltage and volt-watt curve, then the reactive power output will be determined by the nodal voltage and volt-var curve.

To apply the smart inverter setting in the distribution simulation, the PV profile of each PV system is needed. In our study, the loads are measured by the advanced metering infrastructure (AMI), which means that the measurements are the net load; therefore, it is necessary to extract the load profile and PV profile from the AMI load data so that the smart inverter settings can be implemented in each individual PV system.

The contributions of this paper are:

1. We developed a load disaggregation method to extract the load profile and PV profile from the AMI net load measurement so that the smart inverter function can be implemented on the PV systems.
2. We developed a volt-var-watt smart inverter control in Python to fill the gaps in OpenDSS. Currently, the volt-var watt control is not available in OpenDSS, so this function is developed to emulate several advanced smart inverter functions. This function can determine the operating point of the real and reactive power with the nodal voltage, inverter rating, and solar irradiance data as inputs.
3. We simulated the operation of an actual utility distribution feeder with different PV smart inverter settings, and we quantified the performance of each smart inverter setting using statistical results and indexes.

The rest of this paper is organized as follows. Section II describes the models and the data used in this study. Section III introduces the proposed methodologies. The simulation and performance evaluations are shown and analyzed in Section IV. Section V concludes this paper and presents the potential future work.

II. Distribution Feeder Model and Field Data

This section details the distribution feeder modeling and the data sets used in this study.

A. *Feeder Model*

For this study, an actual distribution feeder model developed on the Synergi software platform was received from San Diego Gas & Electric Company (SDG&E). This is a 12-kV feeder that serves approximately 4 square miles of geographic area. The topology of the feeder plotted using the GridPV toolbox [20] is shown in Fig. 1. There is an LTC at the substation transformer and three capacitor banks in the middle of the feeder for voltage regulation and reactive power support. There is one remote terminal unit located in the middle of the feeder measuring the voltage and load data at that node. There are 341 service transformers serving more than 5000 customers. The solar generation of approximately 70% relative to the peak load is present in this feeder at the locations highlighted in Fig. 1.

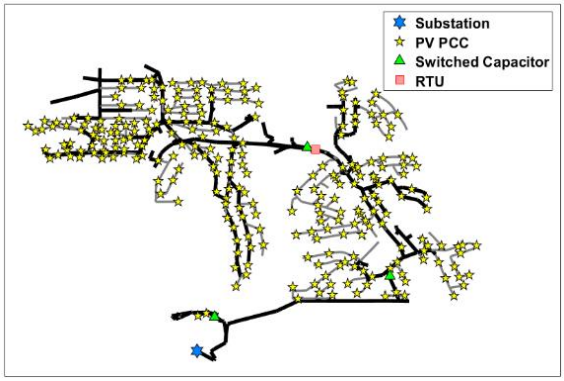

Fig. 1. Topology of the distribution system.

B. *Model Conversion and Validation*

The original feeder model in Synergi is converted to OpenDSS using the Distribution Transformation Tool (DiTTo) model conversion tool [21] so that we can conduct quasi-static time-series (QSTS) simulations required for this study [22]. The converted OpenDSS model is validated by comparing the nodal voltage mismatches between the Synergi and OpenDSS power flow results. The comparison result is shown in Fig. 2. It is observed that the voltage mismatches are low, with all of the mismatches less than 0.006 p.u. This confirms that the model conversion process is accurate.

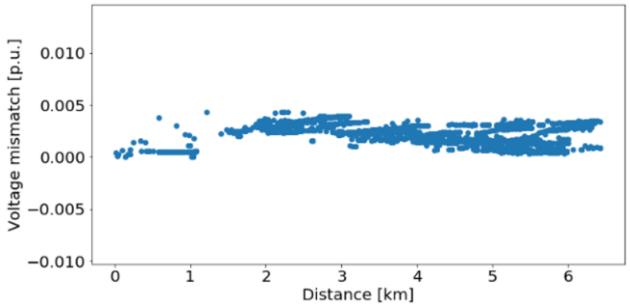

Fig. 2. Bus voltage mismatches between Synergi and OpenDSS power flow results.

C. *AMI Data*

AMI data are recorded at the secondary side of each service transformer in the SDG&E system [23]. The AMI data set includes the real power measurements from two customers and the total real power consumption at the secondary side of each service transformer. Note that the real power measurement is the net load instead of the customers' load consumption, which means that the power from the PV system is already included in the measurement. The AMI data recorded for a period of 107 days from October 2018 to January 2019 are used. The data resolution is 1 hour for the real power measurements at the load locations.

III. Load Disaggregation and PV Smart Inverter Function

A load disaggregation method was used to extract the load profile and the PV profile from the AMI measurements and model the PV systems explicitly in OpenDSS. A volt-var-watt control function was developed in Python to emulate different smart inverter settings for these PV systems in OpenDSS.

A. *Load Disaggregation Method*

Load disaggregation in a distribution system can refer to feeder-head load disaggregation [24], building appliance disaggregation, and load/PV disaggregation. In this study, the AMI load measurements from SDG&E are the net load consumption of each customer; therefore, a load disaggregation method is required to extract the PV profile and the load profile for each load location. From SDG&E's information, the PV penetration in this feeder is 70% relative to the peak load. The solar irradiance profile of the feeder area during the selected period of 107 days is downloaded from the National Solar Radiation Database (NSRDB) website [25]. The relationship between the load and the PV data can be expressed as:

$$P_{load}^{peak} = max\,(P_{net} + 70\% * P_{load}^{peak} * Irradiance), \quad (1)$$

where P_{load}^{peak} is the peak load consumption of the aggregated load profile in the distribution feeder; P_{net} is the aggregated profile of all AMI measurements, which can also be called the total net load curve; and $Irradiance$ is the normalized solar irradiance data from the NSRDB website. The target is to determine P_{load}^{peak} from this equation so that the aggregated PV profile and load profile can both be extracted. As all other values/profiles are known, a P_{load}^{peak} value needs to be find to make this equation satisfy. After iterating over different P_{load}^{peak} values, the equation holds when the peak load is 11012 kW. Based on this number, the aggregated PV profile, P_{PV}, and aggregated load profile, P_{load}, can be calculated by:

$$P_{PV} = 70\% * P_{load}^{peak} * Irradiance, \quad (2)$$

$$P_{load} = P_{net} + P_{PV}. \quad (3)$$

The aggregated PV profile is distributed among all PV systems in the feeder based on the inverter ratings. The nodal load profile at node i is calculated by:

$$P_{load}^{i} = P_{netload}^{i} + P_{PV}^{i}. \quad (4)$$

Because we are focusing on the PV smart inverter functions in this study, a higher PV penetration is preferred; therefore, we increased the PV penetration to 100% by adding extra PV systems to a few randomly selected load locations. This 100% PV penetration scenario is used for the simulations.

B. *Volt-Var-Watt Smart Inverter Function*

In OpenDSS, the volt-var-watt smart inverter control function is not available; therefore, we developed a Python function to implement the volt-var-watt control. The inputs of the function include the smart inverter rating, solar irradiance at the current time step, and the measured voltage at the previous time step. The volt-var and volt-watt curves are predefined first. Then, based on the voltage and volt-watt curve, the function will determine the required real power output, P_{PV}^{i}, at node i by:

$$P_{PV}^{i} = min\,(X\% * S_{PV}^{i}, Irradiance * S_{PV}^{i}), \quad (5)$$

where S_{PV}^{i} is the smart inverter rating of node i, and $X\%$ is determined by the volt-watt curve and the voltage of node i at the previous time step. Then the maximum available reactive power, $Q_{PV}^{i,max}$, at node i can be calculated by:

$$Q_{PV}^{i,max} = \sqrt{{S_{PV}^{i}}^2 - {P_{PV}^{i}}^2}. \quad (6)$$

Then the reactive power output, Q_{PV}^{i}, at node i is calculated by:

$$Q_{PV}^{i} = min\,(Y\% * S_{PV}^{i}, Q_{PV}^{i,max}), \quad (7)$$

where $Y\%$ is determined by the volt-var curve and the voltage of node i at the previous time step. The calculated P_{PV}^{i} and Q_{PV}^{i} will be used to update the PV system output at node i in OpenDSS.

IV. Case Studies

This section presents the PV smart inverter settings used in this study and the simulation results when the settings are applied to the distribution system.

A. *Settings of Smart Inverter Functions*

The following smart inverter settings have been implemented in this study: California Rule 21, Hawaii Rule 14, IEEE 1547, Rule 21 with no deadband, hockey stick with no compensation in the low-voltage region (Hockey Stick 1 or HS1), hockey stick with deeper reactive absorption (Hockey Stick 2 or HS2), and volt-var-watt control. The settings of each smart inverter function are shown in Fig. 3.

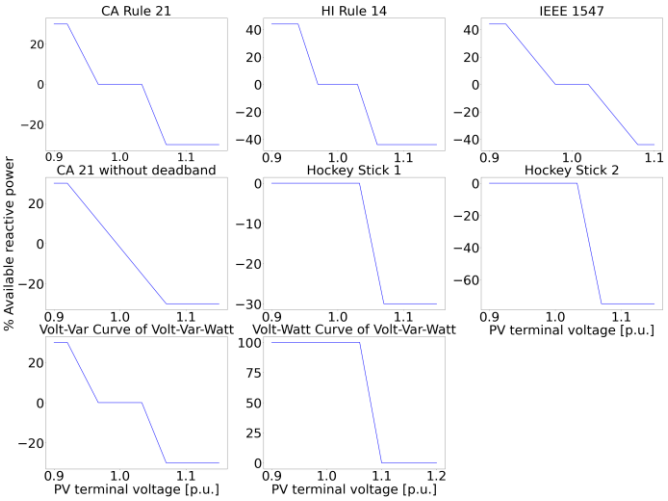

Fig. 3. Settings of different smart inverter functions.

The settings of different smart inverter functions are summarized in Table I. The inverter will output its maximum percentage of available power, Y1, if its voltage is below X1. This percentage is 0 when its voltage is within X2 and X3. The inverter will output its minimum percentage of available power, Y2, if its voltage is above X4. Note that the volt-var-watt setting listed in Table I is its volt-watt curve. The volt-var curve of the volt-var-watt setting is the same as California Rule 21.

Table I. SUMMARY OF DIFFERENT SMART INVERTER FUNCTION SETTINGS

	X1	X2	X3	X4	Y1	Y2
Rule 21	0.92	0.967	1.033	1.07	+30%	-30%
Rule 14	0.94	0.97	1.03	1.06	+44%	-44%
IEEE 1547	0.92	0.98	1.08	1.08	+44%	-44%
Rule 21 no deadband	0.92	NA	NA	1.07	+30%	-30%
HS1	NA	NA	1.033	1.07	0	-30%
HS2	NA	NA	1.033	1.07	0	-75%
Volt-var-watt	NA	NA	1.06	1.1	100%	0

B. *Performance Metrics*

The QSTS simulation is conducted on the distribution feeder with a 107-day load and PV profile. The performance of each smart inverter function is evaluated by multiple metrics: number of capacitor changes, number of LTC changes, average voltage, voltage fluctuation index, voltage unbalance index, voltage exceedances (VE), and number of voltage exceedance nodes (VEN).

Let T stand for the total time steps in the simulation and N stand for the total number of nodes in the feeder, and the average voltage is calculated by:

$$V^{mean} = \frac{1}{N} \times \left(\frac{1}{T}\sum_{i=1}^{N}\sum_{t=1}^{T} V^i(t)\right). \quad (8)$$

The voltage fluctuation index (VFI) is calculated by:

$$VFI = \frac{1}{N} \times \left(\frac{1}{T}\sum_{i=1}^{N}\sum_{t=1}^{T} \left|V^i(t+1) - V^i(t)\right|\right). \quad (9)$$

The voltage unbalance index (VUI) is calculated by:

$$VUI = \frac{1}{N} \times \left(\frac{1}{T}\sum_{i=1}^{N}\sum_{t=1}^{T} V^i_{imb}(t)\right), \quad (10)$$

where $V^i_{imb}(t)$ is calculated by using the maximum deviation from the average voltage over the average voltage.

The voltage exceedance refers to the bus voltage being out of range from 0.94 p.u. to 1.06 p.u. The voltage exceedance node is defined as the node that has more than 12 hours of voltage exceedance during the 107-day period.

C. *Smart Inverter Function Comparison*

This subsection presents the simulation results when the voltage regulation devices are enabled in the distribution feeder. Based on the information from the utility, the capacitor control settings are summarized in Table II. The set point of LTC is 1.025 p.u., and the bandwidth is 2 V with a 120-V base.

Table II. SUMMARY OF CAPACITOR CONTROLS

	On time	Off time	On Voltage	Off Voltage
Capacitor 1	7 a.m.	8 p.m.	0.992 p.u.	1.025 p.u.
Capacitor 2	7 a.m.	8 p.m.	0.992 p.u.	1.025 p.u.
Capacitor 3	NA	NA	0.992 p.u.	1.025 p.u.

To study how the inverter reactive power output changes when applying different rules, the reactive power output from an example PV system is shown in Fig. 4. The baseline of this study is set as the feeder operating without any smart inverters. For the baseline, the reactive power output is 0 because there is no smart inverter enabled. For other rules, the baseline voltages are the starting point before the smart inverter works. Rule 21 without deadband has the highest reactive output because its slope is lower with the voltage changes. The IEEE 1547 and Rule 14 functions have the second and third highest reactive power output, respectively, because they have relatively higher available Q when the voltage is higher. The performance of HS1 is the same as Rule 21 because all the voltages in this distribution system are higher than 0.967 p.u. HS2 has more reactive power output than HS1 because it has deeper reactive power absorption. Therefore, if there are no voltage regulation devices in the system, the rule with more reactive power compensation will solve the voltage problems better. The total energy from substation is also compared for these cases. In general, for each volt-var case, the yearly substation energy difference is +/-0.1% with the baseline case. This is because the real power is not curtailed and the small energy change is from the voltage change along the feeder.

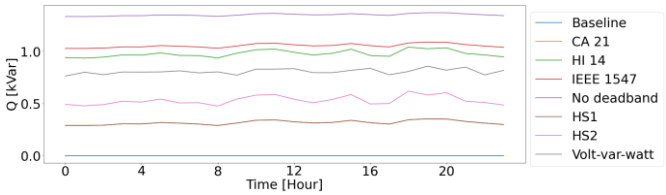

Fig. 4. Reactive power output on an example PV system.

TABLE III. SUMMARY OF FEEDER OPERATION WITH VOLTAGE REGULATION DEVICES ENABLED

	Daily Cap Change	Daily LTC Change	Average Voltage	VFI	VUI
Baseline	5.25	12.07	249.93	9.67	9.90
Rule 21	6.04	12.47	249.20	9.68	9.86
Rule 14	5.03	13.75	248.60	9.67	9.82
IEEE 1547	5.42	13.81	248.66	9.66	9.81
No deadband	5.66	13.03	248.41	9.67	9.77
HS1	6.04	12.47	249.20	9.68	9.86
HS2	5.83	14.07	248.60	9.62	9.83
Volt-var-watt	1.47	7.32	250.27	9.61	9.81

TABLE IV. SUMMARY OF VOLTAGE EXCEEDANCES WITH VOLTAGE REGULATION DEVICES ENABLED

	Secondary		Primary	
	VE hours per node	Number of VEN	VE hours per node	Number of VEN
Baseline	23.52	752	42.83	481
Rule 21	0.55	16	0.61	0
Rule 14	0.21	9	0.76	12
IEEE 1547	0.47	28	0.96	14
No deadband	1.05	37	2.84	42
HS1	0.55	16	0.61	0
HS2	0.09	3	0.91	12
Volt-var-watt	4.45	110	2.95	53

The results for different smart inverter functions are shown in Table III and Table IV. Based on the results from the study, the Rule 21 curve showed superior results in terms of the number of voltage regulation device actions and eliminating the primary voltage exceedances. The Rule 14 curve showed superior results in terms of eliminating the secondary voltage exceedances. The voltage exceedances for the volt-var-watt function are higher than the others, but it has the lowest number of voltage regulation device actions. The numbers of voltage regulation device changes are similar for all other smart inverter functions, and the average voltages are all near 249 V. Based on different purposes of controlling the feeder, the corresponding smart inverter functions can be selected by using the results from this study. For example, if the utility wants to minimize the action times of the voltage regulation devices, Rule 21 can be set for the smart inverters on this

feeder. If the utility wants to eliminate the secondary voltage exceedances, Rule 14 can be implemented in this system.

V. Conclusion

This paper presented a comparison of distribution system operation when different PV smart inverter settings are applied. A realistic feeder model, AMI measurements from the field, and solar irradiance data were used in this study. A load disaggregation method was proposed to extract the load and PV profiles for each load location. A volt-var-watt smart inverter control function was developed in Python to enable the smart inverter setting in the OpenDSS simulation. The widely used PV smart inverter settings were summarized and implemented in the QSTS analysis. The performance of each PV smart inverter setting was summarized, and the analysis of the results can be used by the electric utility to select the best setting on this feeder and to decide how many additional PVs the system can host. The developed simulation platform, smart inverter Python function, and result evaluation criteria can also be used to study other feeders or new smart inverter functions. In our future work, the effectiveness of the load disaggregation method will be studied using actual utility measurements. The impact of PV smart inverter settings with different PV penetration levels, on more utility feeders will be studied, and develop metrics will be developed to quantify the performance.

Acknowledgment

This work is authored in part by the National Renewable Energy Laboratory, operated by Alliance for Sustainable Energy, LLC, for the U.S. Department of Energy (DOE) under Contract No. DE-AC36-08GO28308. Funding provided by U.S. Department of Energy Office of Electricity and by California's Electric Program Investment Charge (EPIC) Program in San Diego Gas & Electric Company under a cooperative research-and-development agreement (CRADA) # CRD-17-712. The views expressed in the article do not necessarily represent the views of the DOE or the U.S. Government. The U.S. Government retains and the publisher, by accepting the article for publication, acknowledges that the U.S. Government retains a nonexclusive, paid-up, irrevocable, worldwide license to publish or reproduce the published form of this work, or allow others to do so, for U.S. Government purposes.

References

[1] D. Gielen, B. Francisco, S. Deger, B. Morgan, W. Nicholas, and R. Ricardo. "The role of renewable energy in the global energy transformation," in *Energy Strategy Reviews*, 24, pp. 38-50, 2019.

[2] B. Uzum *et. al.*, "Rooftop Solar PV Penetration Impacts on Distribution Network and Further Growth Factors—A Comprehensive Review," in *Electronics*, vol. 10, no. 1, pp. 55, 2021.

[3] X. Zhu, J. Wang, N. Lu, N. Samaan, R. Huang, and X. Ke, (2018). A hierarchical vlsm-based demand response strategy for coordinative voltage control between transmission and distribution systems, in *IEEE Transactions on Smart Grid*, vol. 10, no. 5, pp. 48338-4847, 2021.

[4] J. Wang, X. Zhu, D. Lubkeman, N. Lu and N. Samaan, "Continuation power flow analysis for PV integration studies at distribution feeders," *2017 IEEE Power & Energy Society Innovative Smart Grid Technologies Conference (ISGT)*, pp. 1-5, 2017.

[5] S. Wang *et. al.*, "Interval Overvoltage Risk Based PV Hosting Capacity Evaluation Considering PV and Load Uncertainties," in *IEEE Transactions on Smart Grid*, vol. 11, no. 3, pp. 2709-2721, 2020.

[6] California ISO, "Fast facts," 2018. [Online]. Available: https://www.caiso.com/Documents/FlexibleResourcesHelpRenewables_FastFacts.pdf

[7] J. Wang, S. Huang, D. Wu and N. Lu, "Operating a Commercial Building HVAC Load as a Virtual Battery Through Airflow Control," in *IEEE Transactions on Sustainable Energy*, vol. 12, no. 1, pp. 158-168, 2021.

[8] M. Chamana and B. H. Chowdhury, "Optimal Voltage Regulation of Distribution Networks with Cascaded Voltage Regulators in the Presence of High PV Penetration," in *IEEE Transactions on Sustainable Energy*, vol. 9, no. 3, pp. 1427-1436, 2018.

[9] H. A. H. Al-Hilfi *et. al.*, "Estimating Generated Power of Photovoltaic Systems During Cloudy Days Using Gene Expression Programming," in *IEEE Journal of Photovoltaics*, vol. 11, no. 1, pp. 185-194, 2021.

[10] H. V. Padullaparti, M. Lwin and S. Santoso, "Optimal placement of edge-of-grid low-voltage SVCs in real-world distribution circuits," in *IEEE Workshop on Power Elec. and Power Quality Applications*, 2017.

[11] H. V. Padullaparti, Q. Nguyen and S. Santoso, "Advances in volt-var control approaches in utility distribution systems," *2016 IEEE Power and Energy Society General Meeting (PESGM)*, 2016, pp. 1-5.

[12] T. S. Ustun and Y. Aoto, "Analysis of Smart Inverter's Impact on the Distribution Network Operation," in *IEEE Access*, vol. 7, 2019.

[13] P. Jahangiri and D. C. Aliprantis, "Distributed Volt/VAr Control by PV Inverters," in *IEEE Transactions on Power Systems*, vol. 28, no. 3, pp. 3429-3439, Aug. 2013.

[14] H. V. Padullaparti, N. Ganta and S. Santoso, "Voltage Regulation at Grid Edge: Tuning of PV Smart Inverter Control," *2018 IEEE/PES Transmission and Distribution Conference and Exposition (T&D)*, pp. 1-5, 2018.

[15] Rule 21 Interconnection, California Public Utilities Commission, CA, available at https://www.cpuc.ca.gov/Rule21/.

[16] Rule no. 14, Service Connections and Facilities on Customer's Premises , Hawaiian Electric, available at https://www.hawaiianelectric.com/documents/billing_and_payment/rates/hawaiian_electric_rules/14.pdf.

[17] IEEE Standard for Interconnection and Interoperability of Distributed Energy Resources with Associated Electric Power Systems Interfaces, IEEE Std 1547-2018, April 2018.

[18] R. Thiagarajan, P. Gotseff, A. Hoke and E. Ifuku, "Inverter testing for verification of Hawaiian Electric Rule 14H," *2019 IEEE 46th Photovoltaic Specialists Conference (PVSC)*, pp. 0906-0910, 2019.

[19] Rule 21 Generating Facility Interconnections, SDG&E, California, available at http://regarchive.sdge.com/tm2/pdf/ELEC_ELEC-RULES_ERULE21.pdf

[20] M. J. Reno and K. Coogan, "Grid integrated distributed PV (GridPV) version 2," *Sandia National Labs SAND2014-20141*, 2014.

[21] T. Elgindy, N. Gensollen, D. Krishnamurthy, M. Rossol, E. Hale & B. Palmintier. *DiTTO (Distribution Transformation Tool)* (No. DiTTO). National Renewable Energy Lab.(NREL), Golden, CO, 2018

[22] IEEE P1547.7 D5.1 Draft Guide to Conducting Distribution Impact Studies for Distributed Resource Interconnection, IEEE Standard, 2011.

[23] J. Wang, H. Padullaparti, S. Veda, M. Baggu, M. Symko-Davies, A. Salmani, and T. Bialek, "A Machine Learning-based Method to Estimate Transformer Primary-Side Voltages with Limited Customer-Side AMI Measurements," *2021 IEEE Power & Energy Society General Meeting (PESGM)*, pp. 1-5, 2021.

[24] J. Wang, X. Zhu, M. Liang, Y. Meng, A. Kling, D. Lubkeman, and N. Lu, "A Data-Driven Pivot-Point-Based Time-Series Feeder Load Disaggregation Method," in *IEEE Transactions on Smart Grid*, vol. 11, no. 6, pp. 5396-5406, Nov. 2020.

[25] Y. Xie *et. al.*, "Progress on the National Solar Radiation Data Base (NSRDB): A new DNI computation," *2020 47th IEEE Photovoltaic Specialists Conference (PVSC)*, pp. 0330-0332, 2020.